Mech. Adv. Technol. Vol. 6, No. 1, 2022, pp. 41–55

DOI: 10.20535/2521-1943.2022.6.1.260938

UDC 621.54.25

Using the functional approach in the development of hybrid processes in engineering: theoretical base

A.F. Salenko[1] • S.A. Klimenko[2] • V.M. Orel[3] • V.Yu. Kholodny[4] • N.V. Gavrushkevich[1]

Received: 3 May 2022 / Accepted: 30 May 2022

Abstract. *The principles of creating hybrid processing processes based on the functional approach are given. It is proposed to consider the formation of individual elements of the product (planes, holes, fillets, ledges) through functions that are provided by a combination of such elements. At the same time, the required depth of technological influences is analyzed, based on which a set of influences that are different in nature, but compatible, on some basic carrier, is selected. It is proposed to use a high-speed liquid flow as such a carrier. Hybridization of a tool based on a water jet of small diameter can be achieved by combining with laser heating, cryogenic cooling, and the formation of a flow of ice particles, mechanical initiation of surface damage with further development of surface defects. The high efficiency of hybrid processes for processing composite materials is shown.*

Keywords: *Hybrid tool, functional approach, processing of composites, laser processing, jet-laser cutting, cryogenic ice generation.*

Introduction

Traditionally, when creating new products, the range of tasks invested in ensuring the minimum costs for the implementation of the production cycle, ensuring the specified parameters of quality, durability, and reliability. Another block is the issue of ergonomics, environmental friendliness, and recyclability of the product. Somewhat less often the issues of marketing, active promotion of the usefulness and necessity of the product, highlighting its most important competitive advantages are considered.

The experience of recent decades shows that sometimes success in the market is provided by such approaches, which are fundamentally new, non-standard, forcing to attract the attention of consumers. Thus, the manufacturer often encourages the consumer to purchase products; the so-called concept of "activation" or "formation of the need" to purchase this product is implemented, even if the consumer has no obvious need for it.

Until almost 80 years of the last century in the production of material goods dominated by the subject approach. The manufacturer clearly focused on traditions, existing technologies, and the production process itself had an iterative principle, when the finished product, especially complex, underwent several changes based on analysis of its market promotion, consumer feedback, capabilities of equipment, raw materials and materials for its production. Only a little later, with the emergence and development of ideas for a product approach to maximize consumer satisfaction (R. Alderson, R. Cox, V. Cherenkov), the development of methods to enhance creative activity (A. Osborne, T. Busen, G. Altshuller), the emergence and expansion of the use of methods of morphological analysis (F. Zwicky, F. Kunze, D. Jones, Y. Kuznetsov), which allows not only to sort out options for products, but opens new technical solutions that are fundamentally different from existing ones, began to form functional approach. This approach was most systematically developed by E. Golibardov in his theory of functional-cost analysis [1].

Subsequent works by B. Bazrov and A. Mikhailov showed that the previously formulated approaches to the creation of objects of production can be transferred to the

✉ *A. F. Salenko*
salenko2006@ukr.net

[1] *Igor Sikorsky Kyiv Polytechnic Institute, Kyiv, Ukraine*

[2] *V.Bakul Institute for Superhard Materials, Kyiv, Ukraine*

[3] *Kharkiv National University of Internal Affairs, Kremenchuk Flight college, Kharkiv, Ukraine*

[4] *Kremenchuk Mychailo Ostrohradskyi National University, Kremenchuk, Ukraine*

system of technologies. In this case, the production object itself was divided into functional zones of different localization, and methods of work (technological operations) were chosen on the condition of minimizing the cost of their implementation.

The functional approach is based on the premise that the designed object, the process, is considered primarily in terms of the functions for which it is used. Material carriers are discarded at the first stage, and only later, based on the minimum of their value, are selected as the basis for creating a product.

The complexity of products, the use of composite materials in their production necessitates the search for ways to improve the known provisions of the functional approach, considering a number of phenomena of mechanics of composite processing and the possibility of combining power and energy influences. This makes this area of research relevant and meaningful.

Formulation of the problem

Traditionally, during the development of the technological process of preparing a sample (details), it is customary to look at the perfection of the surface or the surface, which includes the successful surface. So, in the process of developing the technological process, assignments of the powers of the elements to the fore at the sight of the superstitiousness of the surface.

At the same time, such consideration does not allow to carry out precisely, subtly, and precisely the set technological influences and to provide necessary properties at local level depending on various features of their operation and action of operational functions. At the same time the technological process is developed, and technological influences are guided during realization of technology for all surface as a whole without taking into account features of action of operational functions. It also does not allow to solve the problem of full adaptation of the properties of the product in the manufacture depending on the peculiarities of its operation.

The authors of [2] propose to introduce detailing the product on several levels, namely: 1st level of division - the level of products, 2nd level of division - the level of functional parts, 3rd level of division - the level of functional components, 4th level of division - the level of functional zones, 5- and the level of division - the level of functional macrozones, the 6th level of division - the level of functional microzones, the 7th level of division - the level of functional nanozones. For composites, the division from the 4th level acquires special significance, as the dimensions of the reinforcements can already be compared with the 5th level of the division.

The block diagram of the implementation of function-oriented technologies for many products will look like this, Fig. 1. Here it is shown: V – product entry; W – output parameters of technology; FE – functional elements; TB – technological implications; 1 - the process of analysis and research №1 (A and №1), which is performed to implement the process of dividing each product into FE according to the levels of depth of technology; 2 - the process of analysis and research №2 (A & I №2), which is performed to combine the FE of each set into a hierarchical structure of subsets depending on the levels of integration.

In this block diagram at the entrance to the system V shows the receipt of the set of products $V = \{1, 2, 3, ..., M\}$. Thus after the analysis and researches of products distribution (decomposition) of each product on FE on levels of depth of technology and drawing up of hierarchical structure of sets of FE on levels of depth of technology is carried out:

$$\left.\begin{aligned} m_1 &= \{f_{11}, f_{12}, f_{13}, ..., f_{1v_1}\}; \\ m_2 &= \{f_{21}, f_{22}, f_{23}, ..., f_{2v_2}\}; \\ m_3 &= \{f_{31}, f_{32}, f_{33}, ..., f_{3v_3}\}; \\ &\cdots\cdots\cdots\cdots\cdots\cdots \\ m_7 &= \{f_{71}, f_{72}, f_{73}, ..., f_{7v_7},\} \end{aligned}\right\} \quad (1)$$

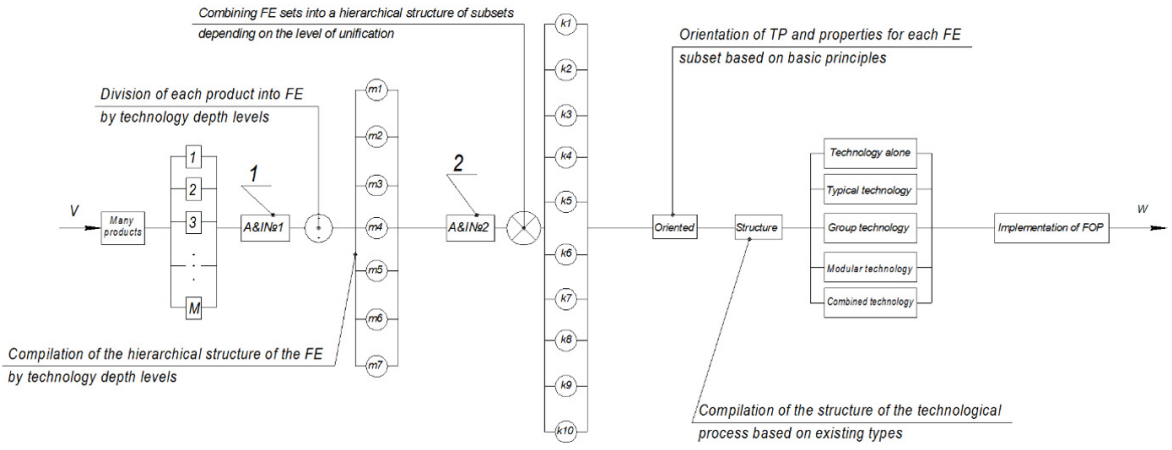

Fig. 1. Block diagram of the implementation of functional-oriented technology for many products (according to [2])

where m_1, m_2, m_3,…, m_7 – sets of functional elements according to the levels of depth of technology; $f_{in} - \eta$ – and a functional element j – level of technology depth, v_1, v_2, v_3,..., v_7 – power or orders of sets m_1, m_2, m_3,..., m_7. The order of sets can be determined by the following formulas:

$$\left.\begin{array}{c} v_1 = M; \\ v_j = \sum_{k_j=1}^{v(j-1)} v_j k_j; \\ j = 2,3,4,...,7, \end{array}\right\},$$

where M – the power of the set m_1 or the number of products (parts) in the analyzed party; $v_j k_j$ – order k_j-th subsets of the j-th level of technology depth; j – technology depth level number. After performing the process of decomposition of each product on the *FE* according to the levels of depth of technology analysis and research of products and combining (composition) of functional elements of each set into a hierarchical structure of subsets depending on the levels of association (10 levels of association):

$$\left.\begin{array}{c} k_1 = \{p_{11}, p_{12}, p_{13}, ..., p_{1u_1}\}; \\ k_2 = \{p_{21}, p_{22}, p_{23}, ..., p_{2u_2}\}; \\ k_3 = \{p_{31}, p_{32}, p_{33}, ..., p_{3u_3}\}; \\ ..... \\ m_{10} = \{f_{101}, f_{102}, f_{103}, ..., f_{10u_{10}},\} \end{array}\right\}$$

where k_1, k_2, k_3,...,k_{10} – set of subsets functional elements, united by the levels of their association; $p_{\varphi\xi}$ – ξ-subset of the φ-th level of association of functional elements; u_1, u_2, u_3, ...,u_{10} – powers or orders of sets k_1, k_2, k_3, ..., k_{10}.

Let a certain element of the product Em be obtained by realizing intermittent technological effects $\prod_{ij}^{t}$ and $\prod_{ij+k}^{t}$. It can be expected that this requires k tools. However, if we consider that the creation of a new tool is based on known, ie. $R_{nj} = \bigcap_{i=1}^{p_i} R_{si}$, R_{nj} – field of formations of new types of tools; R_{si} – i-th set of known technical solutions; ρ_i is the weight of a subset of known solutions, then the newly obtained tool can combine into one whole means for fundamentally different types of impact.

Thus, the set of properties of two instruments are expressions

$$I_1 = \begin{Vmatrix} \rho_{11} S^1_{11} & \rho_{21} S^1_{21} & \rho_{k1} S^1_{k1} \\ ... & ... & ... \\ \rho_{1j} S^1_{1j} & \rho_{2j} S^1_{2j} & \rho_{kj} S^1_{kj} \end{Vmatrix},$$

$$I_2 = \begin{Vmatrix} \rho_{11} S^2_{11} & \rho_{21} S^2_{21} & \rho_{k1} S^2_{k1} \\ ... & ... & ... \\ \rho_{1j} S^2_{1j} & \rho_{2j} S^2_{2j} & \rho_{kj} S^2_{kj} \end{Vmatrix}. \qquad (2)$$

Then the hybrid tool obtained on the basis of the principle of morphological search and combining properties will consist of elements, and $m < k + j$, because part of the properties of the original tools can be combined. Thus, the hybridization rate of the created tool $k_g = \frac{k+j}{m}$. This indicator makes it possible to find rational technical solutions for hybrid tools based on the set of required properties of the workpieces, as well as the ability to achieve them with available tools.

The purpose of the work

Is to substantiate the expediency of using a functional approach to the development of processes that use a hybrid tool to perform technological operations with composite materials.

The main content of the work

The hybrid tool at formation of functional elements of a product of *FE* forms not only useful properties of a product. After all, from the point of view of the functional approach, the formation of the useful function F_p usually occurs with the formation of neutral F_n and harmful F_v functions. Then the condition of an ideal product is $F_p = F_{pz}$, $F_v = 0$, $F_n \to \min$, where F_{pz} is the task of useful properties of the product.

In general, the properties of the product because of the implementation of the treatment process (its physical and mechanical characteristics, geometric parameters, etc.) are expressed as follows:

$$P = \sum_{i=1}^{l} F_{pi} + \sum_{j=1}^{m} F_{nj} + \sum_{k=1}^{p} F_{vk} .$$

These equations allow us to search for rational material carriers of functions and methods for obtaining them. The ratio of useful and harmful functions or manifestations of the process is written as $F_v = pF_p$, $F_n = qF_p$. So $P = \sum_{i=1}^{l} F_{pi} \left(W_p + \overline{W_p} q + \overline{W_p} p\right)$. Approximation of a product with a set of FE_i, giving the properties of P to the ideal, involves the reversal of applications $\overline{W_n} q$ and $\overline{W_v} p$ to zero, which is possible provided there is no functional relationship between useful and harmful properties of the product or provided that the process useful functions of the accepted material carrier at the same time is inverse to the emerging harmful functions. The presence and relationship between the individual elements of the technological process allows us to represent the expression for P as follows:

$$P_v = \sum_{i=1}^{l} F_{pi} (b_{ki} W_{pi} - b_{vi} \overline{W_{pi}} p - b_{ri} \overline{W_{pi}} (p + q))$$

provided that $b_{ni} \overline{W_{pi}} q = 0$, b_{ki} – the corresponding weights of each of the useful functions; b_{vi} – weighting factors of each harmful function (subtracting component); b_{ri} – weights of interaction of independent transitions, which reveal reserves in improving the initial properties of the finished product.

Therefore, a possible combination of options for forming the elements of the product by certain instrumental influences can be represented in table 1.

Table 1. Possible combinations of impact options and their depth

Depth of separation levels						
7						
6						
5						
4						
3						
2						
Functional elements	Options for execution					
	M_r	M_d	L	WJ	Ab	Cr
FE_1 Π^t_{ij}	$\delta^{p1}{}_t, \Delta^{l1}{}_i, h_\sigma, l_j$	$\delta^{p2}{}_t, \Delta^{l2}{}_i, h^2{}_\sigma, l_j$	$\delta^{p3}{}_t, \Delta^{l3}{}_i, h^3{}_\sigma, l_j$	$\delta^{p4}{}_t, \Delta^{l4}{}_i, h^4{}_\sigma, l_j$	$\delta^{p5}{}_t, \Delta^{l5}{}_i, h^5{}_\sigma, l_j$	$\delta^{p6}{}_t, \Delta^{l6}{}_i, h^6{}_\sigma, l_j$
FE_2 Π^t_{ij+k}		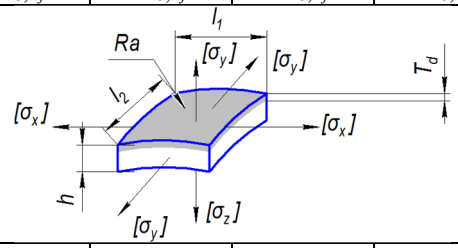				
FE_3 Π^t_{ij+k} Π^t_{i+1j+1}	.....					.....
.....	.....					.....
FE_k	$\delta^{pk1}{}_t, \Delta^l{}_i, h^{k1}{}_\sigma, l^{k1}{}_j$	$\delta^{pk2}{}_t, \Delta^2{}_i, h^{k2}{}_\sigma, l^{k2}{}_j$	$\delta^{pk3}{}_t, \Delta^3{}_i, h^{k3}{}_\sigma, l^{k3}{}_j$	$\delta^{pk4}{}_t, \Delta^{l4}{}_i, h^4{}_\sigma, l^{k4}{}_j$	$\delta^{pk5}{}_t, \Delta^l{}_i, h_\sigma, l_j$	$\delta^{pk6}{}_t, \Delta^{lk7}{}_i, h_\sigma, l_j$

Here it is marked: M_r – mechanical cutting; M_D – mechanical dynamic load; L – laser exposure; WJ – water-jet effect; Ab – abrasive effect; Cr – cryogenic influence. Also shown are not only the possibility of forming the parameters of certain functional surfaces FE_i, but also the depth of coverage of the instrumental influence of the elements of the product at separation levels 1–7.

Now k compositions of tools can appear as parameters of functional action: productivity Q_{FE}, accuracy $\Delta_i{}^{lk}$, rigidity Ra_{FE}, destruction, etc. Let's choose the resulting factors of means of influence on the functional elements of FE_i as a set (or set) of properties of tools $\boldsymbol{I}$.

Then the model of influence on the processed material (composite) is built based on the physical nature of the influences. Consider Fig. 2, it becomes obvious that the hybridization of the instrument is not limited to a comprehensive change in the conditions for the formation of means of active influence. Indeed, the introduction of abrasive particles (1), the addition of cryogenic fluid (2), the combination with the laser beam (3) provide fundamentally new properties of the means of action, as well as radically change the phenomena in the interaction zone, resulting in new opportunities.

The action can also occur when the flow in some way creates the conditions for attracting, for example, the mechanical action of the elements of the elastic system (4), Fig. 2, as well as by providing certain effects on the workpiece (when creating, for example, dynamic initiation by ultrasonic action zones of influence (6), [3] As follows from Fig. 1, this action can be directed both from the jet (1–4) and from the workpiece (5, 6).

To find a rational solution to a hybrid tool, it is advisable to use its functional-cost model (FCM), which is suitable for identifying both desirable and unnecessary (unnecessary) functions and elements (unnecessary and harmful); determining the functional sufficiency and usefulness of the elements of the object; distribution of costs by function; assessments of the quality of performance of functions; detection of defective functional zones in the object; determining the level of functional and structural organization of the product. Construction of FCM is carried out by combining FM and PM object.

Assessment of the significance of the function is carried out sequentially on the levels of FM (top to bottom), starting from the first level. For the main and secondary, i.e., for the external functions of the object, when assessing their significance, the initial distribution of consumer requirements (quality indicators, parameters, properties) by importance (importance). The normalizing condition for determining the significance of a function is the following condition: $\sum_{j=1}^{n} r_{ij} = 1$,where r_{ij} – significance of the j-th function belonging to this 1st level of FM (determined by experts), $j = 1, 2, ..., n$, n – the number of functions located at one level of FM and belong to the general object of higher equal. For internal functions, the determination of significance is based on their role in providing higher-level functions.

Considering the multi-stage structure of FM, together with the assessment of the significance of functions in relation to the nearest higher function, determines the

relative importance of the function of any *i*-th level *R*ij in relation to the product as a whole:

$R_{ij} = \prod_{i}^{G-1} = r_{ij} \times r_{(i-1)(j-1)}$, where G – number of FM levels.

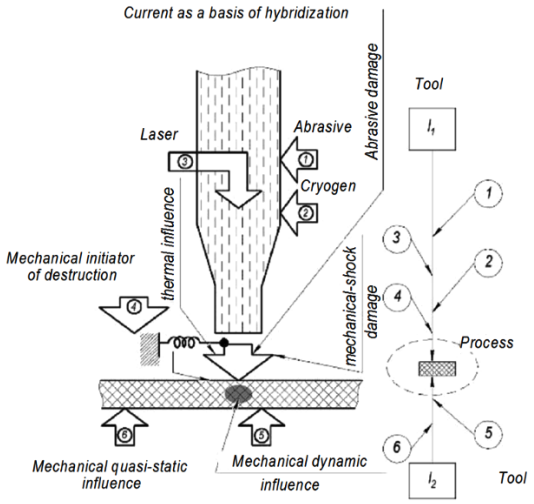

Fig. 2. Hybridization of action based on jet exposure

If one function participates simultaneously in providing several functions of the highest level of FM, its significance is determined for each of them separately, and the relative importance of the function for the object is calculated as the sum of R_{ij} values for each branch of FM (from the 1st level to the first), passing through this function.

The generalized (complex) quality indicator of the variant of performance of functions is estimated by the following equation: $Q_v = \sum_{j=1}^{n} R_j \times P_{jv}$ where R_i – the relative importance of the *j*-th function; P_{jv} – measure of satisfaction (performance) of the *j*-th function in the *v*-th mode; *n* is the number of functions.

Table 2. Components for building a functional-cost model

Function index	The material carrier of the function	The name of the function	Significance of the function [*r*]	The relative importance of the function [*R*]	Degree of function satisfaction [*P*]	Quality of function performance [*Q*]	The absolute cost of the function [$S_{абс}$]	Relative value of function implementation [$S_{відн}$]
1	2	3	4	5	6	7	8	9
1 … *n*	m_1 … m_j	F_1 … F_k	r_{11} … R_{ij}	R_{11} … R_{ij}	P_{11} … P_{jv}	Q_1 … Q_v		

The degree of performance of functions (***P***) is determined on the basis of experimental studies in the percentage listed in the share (from 0 to 1, where 1 is the maximum degree of satisfaction). Functionally necessary costs - the minimum possible costs for the implementation of a set of functions of the object in compliance with the requirements of consumers (quality parameters) in terms of production and use (operation), organizational and technical level of which corresponds to the complexity of the designed object.

The absolute cost of implementation of functions (S_{abs}) is determined as follows:

$$S_{abs} = S_{vig} + S_{\exp} + S_{mp} + S_{en} + S_i$$

where S_{vig} – costs associated with the creation or modernization of the object under study; S_{exp} – operating costs; S_{mp} – costs associated with the complexity of the function; S_{en} – energy consumption for the implementation of the function; S_i – other costs for the implementation of the function.

Relative cost of realization of functions S_r: $S_r = \dfrac{S_{absFij}}{\sum_{1}^{n} S_{abs}}$

where S_{abs} – the total absolute value of the operation of the object is determined by summing the values of the absolute costs of implementation of functions (column 8 in table 2). Based on the comparison of these diagrams in the basic and proposed versions, we can conclude about the degree of usefulness and economic feasibility of the proposed technical solutions of the hybrid tool. The above is explained in Fig. 3.

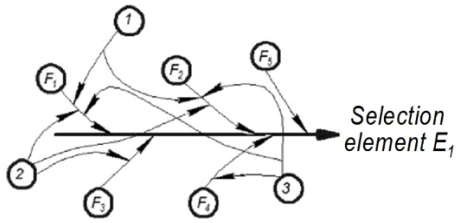

Fig. 3. Providing functions with a set of properties of the hybrid tool

Here it is marked: F_1 – formation; F_2 – the formation of a destructive layer; F_3 – heating; F_4 – cooling; F_5 – localization; F_6 – reproducibility, etc.

Jet effect as a hydrodynamic action (based influence)

Jet technology is based on the use of the potential energy of a compressed liquid flowing from a small-diameter nozzle at supersonic speeds to carry out the work of breaking a solid body. Compressed fluid, flowing from the nozzle, acquires kinetic energy of motion, and if the hydrodynamic pressure on the barrier - the workpiece, the yield strength, begins to form a funnel of destruction. The speed of development of the funnel is determined by a number

of factors, in particular, the conditions of jet formation, its compactness, physical and mechanical properties of the workpiece, etc.

The formation of the groove of the cut, in which the funnel of destruction grows, is always accompanied by the appearance on the surface of a destructive (destroyed, with broken integrity, but not separated) layer. Its occurrence is due to the sequential movement of a certain amount of material from the zone in which technological factors (jet pressure, fluid flow rate, jet compactness), physical and mechanical properties and structure of the material, manifestation of high frequency load and Rebinder effect, and parameters of jet equipment cause the origin of microcracks, their concentration and probable directions of propagation, to the zone of maximum load, in which the active dispersion of the body is a consequence of branching and merging of microcracks with subsequent removal of destruction products from the cutting zone.

The scheme of interaction of a fast-flowing stream of small diameter with the processed material is presented in fig. 4.

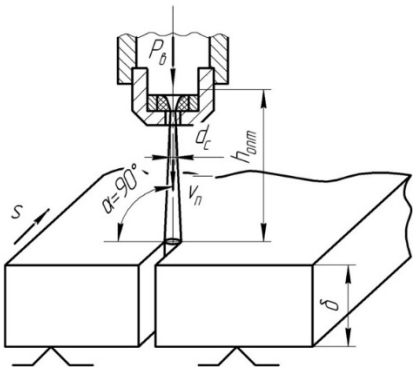

Fig. 4. Interaction of small-diameter rapid flow with the treated material

Providing feed motion with velocity *s* and the existence of a certain velocity v_p deep into the workpiece leads to the fact that at the front of the cutting zone elements of the separation surface are oriented at certain angles зростання, increasing which causes increased hydrodynamic load on the side surface of the cutting zone. The maximum angle of inclination is, and a decrease in the amount of recess *h* and jet into the body with increasing feed s leads to a sharp deterioration in the quality of the separation surface.

Typically the profile can be determined using the Havier-Stokes equation for the conditions of fluid flow along a certain nozzle profile, taking into account the continuity equation $\frac{\partial p}{\partial t} + div\left(\rho \vec{W}\right) = 0$, where $\vec{W}$ – velocity vector, ρ – fluid density, *t* – time, *p* – pressure.

Deformation of materials in horizontal *U*(*t*) and vertical planes *H*(*t*) determined by the equations of stress and strain ratios (provided the direction of the axis in the direction of flow of the jet:

$$\sigma_r = 2G\left(\frac{\partial U}{\partial r} + \frac{\mu\varepsilon}{1-2\mu}\right);\ \sigma_\tau = 2G\left(\frac{U}{r} + \frac{\mu\varepsilon}{1-2\mu}\right);$$

$$\sigma_я = 2G\left(\frac{\partial H}{\partial z} + \frac{\mu\varepsilon}{1-2\mu}\right);\ \tau = G\left(\frac{\partial H}{\partial z} + \frac{\mu\varepsilon}{1-2\mu}\right).$$

Here is $\varepsilon = \varepsilon_r + \varepsilon_t + \varepsilon_z = \frac{\partial U}{\partial r} + \frac{U}{r_m}\frac{\partial H}{\partial z}$,

compatibility condition $\begin{cases} (1-2\mu)\left[\Delta U - \frac{U}{r_m^2}\right] + \frac{\partial \varepsilon}{\partial r} = 0; \\ (1-2\mu)\Delta U + \frac{\partial \varepsilon}{\partial r} = 0 \end{cases}$

$\Delta = \frac{d^2}{dr^2} + \frac{d}{r\partial r} + \frac{d^2}{\partial z^2}$ – Laplace operator, and

$$\varepsilon = \frac{1-2\mu}{2(1-\mu)G}\left(\sigma_r + \sigma_t + \sigma_z\right) = \frac{1-2\mu}{E}\left(\sigma_r + \sigma_t + \sigma_z\right).$$

Hydro cutting composite material with maximum productivity (maximum allowable feed under the condition of complete cutting of the workpiece section) allows to determine the initial angle of the elementary fracture planes as a function of changing the rate of deepening of the jet on a stronger layer: $\alpha = \arctan\left(2r / h(v_c / v_0)\right)$, moreover $v_z, v_0 = f(T) = (p-T)r_c^2 v_c / Tr^2$. In the formulas: *r* is the radius of the jet, *h* is the wall thickness of the product, v_s, v_0 is the rate of penetration of the jet into the material, *p* is the pressure of the process fluid, $T = T_m$ is the strength of the material, v_c is the flow rate of the jet, and $T = T'_m$ – strength of reinforcing inclusions (if the composite is cut). To completely cut the material, the feed rate s_{pk} relative to the treated surface must be reduced to a level

$$s_{pk} = s\frac{hM}{h + x(M-1)};\quad M = \frac{(p-T_m)T'_m}{(p-T'_m)T_m} \qquad (5)$$

s – feed, calculated for the case of cutting a homogeneous material with a tensile strength equal to the tensile strength of the composition as a whole; *x* is the structure parameter.

Mechanical action of jet-abrasive (1)

It is known [4] that the destruction of the material under the action of jet-abrasive flow occurs due to polydeformation damage to the surface with the simultaneous destruction of the abrasive particle. This phenomenon is characteristic of the conditions of inflow of hydroabrasive jet at angles close to normal (i.e. for cases where there is no through cut, and particles bombard the surface, causing individual microdeformations and activating the emergence and development of initial microdefects). The destruction of the material, the origin and development of the hydrocutting hole is possible by microcutting, but in this case, surface defects due to the initial elastic deformation at the point of impact of the particle are possible only when

changing the vector of particle motion. In other words, the micro-risk is formed by the particle now when, hitting the surface, it changes the direction of movement under the action of liquid rapid flow and is removed from the zone of influence. Of course, the intensity of removal remains very low, because the kinetic energy reserve of the particle is significantly reduced.

According to the law of conservation, we have: $\vec{v_b}dm_b + \vec{v_a}dm_a = \vec{v}(dm_b + dm_a)$. Then the velocity of the jet element at the time of entry of the microvolume of nitrogen into the jet will be $\vec{v} = \dfrac{\vec{v_b}dm_b + \vec{v_a}dm_a}{dm_b + dm_a}$.

Since the flow rate of the particles is almost zero, $v_a = 0$ (Fig. 5), after partial braking of the flow, its speed will be $\vec{v} = \dfrac{\vec{v_b}dm_b}{dm_b + C_a dm_a}$ where Ca – coefficient taking into account the active inhibition of the flow of the liquid phase of nitrogen at the time of entry into the fluid flow, $dm_b = \rho v_b \pi r_b^2 d\tau$, ρ – conditional density of liquid; $d\tau$ is the period of time during which the cross section of the jet moves by a distance dl; r_b is the radius of the flow at the time of mixing. This radius is determined by the distance X from the cut of the nozzle and for the catenoid profile (which have used sapphire nozzles) is [5] $r_b = 0.1625\sqrt{d_z X}$. For classical systems of mixing of abrasive with fast flow by means of the mixing chamber (supply of particles carried out by ejection of air-abrasive flow) the distribution of particles by cross section is in accordance with the law

$$M_c = \int_0^t m \cdot f \cdot dt = \frac{f}{(y_{i+1} - y_i)(z_{i+1} - z_i)} \int_0^t Q_m P(D(y,z))dt,$$

where $P(D(y,z)) = \int_{y_i}^{y_{i+1}} \int_{z_i}^{z_{i+1}} a(y,z)dydz$ – the probability of a particle hitting a specific point of intersection,

$$P(D(y,z)) = \frac{1}{2\pi\sigma_y\sigma_z} e^{-\frac{(y-a_y)^2}{2\sigma_y^2} - \frac{(z-a_z)^2}{2\sigma_z^2}} \quad (6)$$

where a_y, a_z – scattering centers (mathematical expectations) along the OY and OZ axes, respectively; σ_y, σ_z – standard deviations y, z – variable coordinates. In this case, according [5] the effective diameter of the jet is

$$\frac{w_e}{d_n\sqrt{R}} = 0.0335\sqrt{\frac{X}{X_c}}\left[1 - \sqrt{\frac{\sigma_c}{2P_1}\frac{X}{X_c}}\right]^{2/3}.$$

The mechanism of interaction of abrasive particles with the processed material is based on the creation of local high-intensity loads by particles, which lead to some elastic-plastic micro- and macro-deformations of compression in local volumes of the surface layer. For example, as we showed in [6], which evaluates the possibility of hydroabrasive treatment of hard alloys of the group TK and BK on the Co bond, these loads are absorbed mainly by the carbide skeleton of the material. Further pickup of abrasive particles by the fluid flow relieves the load, resulting in partial elastic recovery of the deformed volume of the surface material with the appearance of local tensile stresses, which leads to redistribution of stresses between the components of the material.

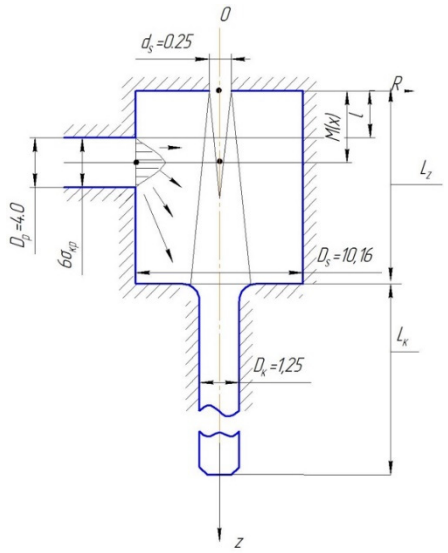

Fig. 5. The diagram of the formation of hydroabrasive flow

Each particle, hitting the surface of the channel at angles within π/2… π/4, will cause elastic-plastic deformation of the surface layer, and going at sharper angles less than π/6… π/12, will form burrs on the surface, which in the future may become centers of origin and development of macrodefects. Based on the analysis of the interaction of particles with the flow along the slice of the jet nozzle and the assumption of hole-like deforming-microcutting fracture, the possible volume W_z of extracted material from the channel surface for time τ is determined, which will be:

$$W_z = \left(\frac{\pi\delta_n{}^2(3r - \delta_n)}{3} + \sqrt{r^2 - (r - \delta_n)^2}\,\delta_a\delta_n\right)\frac{M_a}{m}\tau \quad (7)$$

where M_a – mass abrasive consumption; δ_n – pressing the particle into the surface, δ_a – contact area length:

$$\delta_n = \frac{R_a m \sin\varepsilon_i}{2k_n z_n H_V}\left(K\left(\frac{L}{Z_c}\right)^{\frac{4}{3}}\frac{2\mu p_b}{\sqrt{2p_b\rho} + \frac{M_a}{f_k}}\right)^2;$$

$$\delta_a = \frac{mz_n\cos\varepsilon_i}{2k_a\sigma_b}\left(K\left(\frac{L}{Z_c}\right)^{\frac{4}{3}}\frac{2\mu p_b}{\sqrt{2p_b\rho} + \frac{M_a}{f_k}}\right)^2 - \frac{k_a T_p^2 \sigma_b R_a}{2mz_n}, \quad (8)$$

where m – mass of abrasive particles; R_a, H_V, σ_b – parameters of surface roughness, hardness and strength; z_n – granularity of abrasive particles; r – particle radius; L – the length of the calibration tube; Z_c – the distance from the nozzle cut to the treatment surface, $Z_c = L + \Delta$; K – proportionality factor, which takes into account the ratio of the diameters of the nozzle and the calibration tube, as well as the consumption and dispersion of the abrasive; p_b – pressure in front of the jet nozzle; ρ – fluid density; μ – nozzle consumption factor; M_a – mass consumption of abrasive; f_k – the area of contact of the jet with the obstacle $f_k = \frac{\pi d_c^2}{4}$, T_p – constant, taking into account the inertia of the microcutting process; ε_i – the angle of the particle after interaction with the shell of the jet, which is determined by the angles α_i and φ_i.

Mechanical (shock-dynamic) effect is used mainly to intensify the treatment process. This effect intensifies the active growth of the initial defects that exist in the surface layer.

In the paper [7] it is noted that for the intensification of surface defects it is possible to use mechanical action, which is carried out, for example, by concentrated masses (balls) mounted on elastic suspensions and in contact with the treated surface. Energy for the oscillating motion of such an elastic ball system is obtained from external sources (for example, from a transient flow).

Flowing from the nozzle, the jet also affects the concentrated masses in the form of balls mounted on elastic suspensions. In the first approximation, a hydrodynamic force will act on the ball under the condition of continuous flow $F = \frac{c_x \omega \rho_p V^2}{2} \omega = \frac{\pi d^2}{4}$ – the area of the ball in the midsection, $c_x = \frac{4}{3} \frac{gd}{v_0^2} \frac{\rho_m - \rho_h}{\rho_p}$ – drag coefficient, d – diameter of balls. The equation of motion of the ball on the elastic suspension will have the form:

$$m_i \frac{d^2 x_k}{dt^2} - v_k \frac{dx_k}{dt} - c_1 x_k = F .$$

A stream that interacts with a cryogenic fluid (2) and shock-dynamic influences (4)

The supply of liquid nitrogen from the thermos is carried out in the mixing chamber, which may be like the chamber of Fig. 6. It is more expedient to do it in an adjustable ring nozzle, according to [8]. Since we used a ring nozzle with two conical coaxial tubes, we will use the following considerations to determine the velocity distribution in the closing channel flow. The flow of viscous fluid through the passage of the channel with the z-axis provide

$$du \frac{\partial u_x}{\partial x} \approx 0 \text{ is } -\frac{1}{\mu} \frac{\partial p}{\partial x} + \frac{1}{r_i} \frac{\partial}{\partial r_i} \left(r_i \frac{\partial u_x}{\partial r_i} \right) + \frac{1}{r_j} \frac{\partial^2 u_x}{\partial \theta^2} = 0 .$$

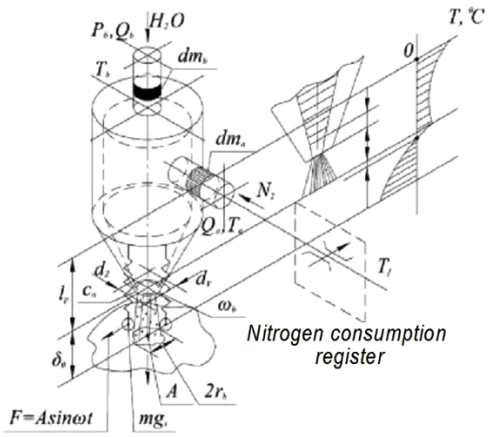

Fig. 6. Formation of water-ice flow by a tubeless device

The flow rate of the inlet is determined as follows:

$$Q = \frac{\pi}{8\mu} \frac{\partial p}{\partial x} \left[b^4 - a^4 - \frac{\left(b^2 - a^2 \right)^2}{\ln\left(b / a \right)} \right].$$

Then, under the condition of continuous flow, $q = Q$ and, accordingly, the flow rate of liquid nitrogen (N_2) will be

$$u = \frac{\pi}{2\mu \left(b^2 - a_3 \right)} \frac{\partial p}{\partial x} \left[b^4 - a^4 - \frac{\left(b^2 - a^2 \right)^2}{\ln(b / a)} \right] \qquad (9)$$

The supply of liquid nitrogen can be carried out by one channel or several channels simultaneously. Depending on the method of fluid supply, the mode of movement will change, and in case of asymmetry of the supply, the flow will be twisted. In this case, the flow regime will change, therefore, the fractionality of the generated ice and the geometric parameters of the flow conditions on the treated surface will change. The movement of liquid nitrogen in the tangential direction in the borehole in front of the channel of the conical nozzle can be described on [8] so: $\rho w_x \frac{\partial w_x}{\partial x} + \rho w_r \frac{\partial w_r}{\partial r} = -\frac{\partial p}{\partial x} + \frac{1}{r} \frac{\partial (\tau r)}{\partial r}$; $_r \frac{\partial p}{\partial r_0} = \rho \frac{\partial w^2}{\partial x}$; $\frac{\partial (w_x r_0)}{\partial x} + \frac{\partial (w_x r_0)}{\partial r_0} = 0$ where w_x, w_r – velocity of fluid in the radial and axial directions, ρ – density of liquid nitrogen.

Under the condition of rotational motion with asymmetric supply of liquid nitrogen, the distribution of tangential stresses in the turbulence zone based on the Prandtl hypothesis can be described as: $\tau_\varphi = \rho l_\varphi^2 \left[\frac{1}{r} \frac{\partial \left(w_\varphi r \right)}{\partial r} \right]^2$ and the relative coefficient of friction depending on the angle φ_w the flow twist will change as follows:

$\psi = \frac{\sqrt{1+\left(\frac{1}{\cos\varphi_w}-1\right)^{4/3}}}{\cos\varphi_w}$, l_φ – the length of the path, in the first approximation the distance to the end of the channel.

Coefficients of friction in the respective directions *r* and x c_x and c_r are $c_i = 0,0256\frac{1}{\mathrm{Re}_i''}$ moreover $\mathrm{Re}'' = \frac{w_i\delta_i}{v}$.

Therefore, based on [9], the integral relation connecting the modes of fluid motion in front of the conical nozzle with the conditions of fluid supply will have the form:

$$\frac{d\,\mathrm{Re}_x''}{dx} = \frac{c_{fx}}{2}Rw_0 - (1+H)\frac{\mathrm{Re}_x''}{w_0}\frac{dw_0}{dx} + \\ +(1-\frac{\delta_x}{2r_0})\frac{R}{2}\frac{\delta_x}{r_0}\frac{1}{w_0}\frac{dw_0}{dx} \quad (10)$$

The thickness of the boundary layer, the distribution of velocities and pressures in the flow of the conical annular nozzle will be determined by the conditions of twisting of the flow due to several channel supply of liquid nitrogen nozzle.

Under the pressure on the free surface of the thermos with liquid nitrogen equal to atmospheric p_a, nitrogen consumption will be $q = \mu f_d\sqrt{\frac{2(p_a-p_k)}{\rho}}$, then $dm_a = qd\tau = \mu f_d d\tau\sqrt{\frac{2(p_a-p_k)}{\rho}}$, with a slight deceleration of the flow.

Heat exchange occurs when mixing flows, due to the active movement of liquids between them. The flow of fluid is considered homogeneous only in the core of the jet, in areas near the periphery – it is the flow of the discrete phase (the movement of individual droplets). When the liquid leaks, there is a nonstationary thermal conductivity, which in the first approximation can be described by the corresponding equation: $\frac{\partial T}{\partial\tau} = aL(T) + f(\Delta T)$, $a = \frac{\lambda_h}{c_h\rho_h}$, $f(\Delta T_h) = \frac{q_+ - q_-(\Delta T_h)}{\delta_a c_h\rho_h}$, $L = \frac{\partial^2}{\partial x^2} + \frac{1}{r_z}\frac{\partial}{\partial r}$, T_h – water temperature when passing through the nozzle, ΔT_h – temperature pressure; λ_h – thermal conductivity, c_h – heat capacity, ρ_h – density, δ_h – thickness, *x* – coordinate along the contact surface of fluid flows. Heat dissipation intensity *q* modeled according to the recommendations [10]; when modeling heat absorption, water was considered when cooling from the initial temperature T_h leakage from the nozzle, changed its physical state at T_i = 273 K then the ice cubes were cooled to temperature $T_к$.

The total energy of the analyzed system, taking into account the variable heat balance of mixing due to the release of energy (heat) of crystallization, was determined based on the results obtained [10]:

$$(1-a)\left(T\frac{dC_p}{dx} + C_p\frac{dT}{dx} + V\frac{dV}{dx}\right) + \\ +a\left(\left[\sum_{i=1}^{N} c_i g_i\frac{dT_i}{dx}\right] + \left[\sum_{i=1}^{N} T_i g_i\frac{dC_i}{dx}\right] - 3aq\sum_{i=1}^{N}\xi^2{}_i\frac{d\xi_i}{dx}\right) + \\ +a\sum_{i=1}^{N} V_i\frac{dV_i}{dx} = T_0\left[(1-a)\frac{dC_p}{dx} + a\frac{dC_i}{dx}\right];$$

$$\frac{dC_p}{dx} = \frac{dC_i}{dT}\frac{dT}{dx}; \quad \frac{dC_i}{dx} = \frac{dC_i}{dT_i}\frac{dT_i}{dx},$$

where α, g_i – total mass fraction and fraction of i-th (by mass) fractions in the total mass of the discrete (ice) phase in the flow; *T*, *V*, T_i, V_i – values of temperature and velocity of gas and *i*-th ice particles, respectively; *q*, ξ_i – latent heat of change of phase state of discrete phase substance and current value of degree of crystallization of *i*-th fraction; T_0 – critical gas braking temperature, °C; C_p,C_i the value of the specific heat of the gas and *i*-th discrete phases, respectively.

The action of the laser as a spot heater with cooling (3)

Heating of the surface by laser radiation is sufficiently studied. It is believed that the temperature distribution is satisfactorily described by the expression

$$dT(x,y,z,t) = \frac{\delta q}{\rho C(4\pi a(t-t'))^{3/2}}\times \\ \times\exp\left[-\frac{(x-x')^2+(y-y')^2+(z+z')^2}{4a(t-t')}\right].$$

For a point with coordinates (*x*, *y*, *z*) for time *t* if warm δq will instantly reach a point on the surface that has coordinates (*x* ', *y*', *z* ') and time *t*'; *C*– heat capacity, α – diffusion, ρ – density, *K*– thermal conductivity. The formulation of the thermal problem for the case of leakage of liquid with radiation on a normally oriented surface is as follows. The flow of liquid is a refrigerant that is fed directly to the laser zone. The equation proposed by [8] can determine the temperature fields in the case when the coolant - ultra-high pressure fluid is not supplied:

$$T(x,y,z) = \frac{P}{\pi^{0.5}\rho c}\int_0^l \frac{e^{\frac{(x-v(t-z))^2}{4a\tau+A^2}\frac{y^2}{4a\tau+D^2}}}{\left[\left(4a\tau+A^2\right)\left(4a\tau+B^2\right)a\tau\right]^{0.5}}\times \\ \times\left[e^{-\frac{z^2}{4a\tau}} - h(\pi a\tau)^{0.5}erfc\left(\frac{z}{2(a\tau)^{0.5}} + h(a\tau)^{0.5}\right)e^{hz+h^2a\tau}\right]dt \quad (11)$$

where ρ, c, λ – density, specific heat, and coefficient of thermal conductivity of the material, respectively; $a = \frac{\lambda}{cp}$ – thermal conductivity of the material; h – heat transfer coefficient from the surface; A and B – larger and smaller semi-axes of the elliptical beam; $P = q\pi AB$ – power of the laser emitter.

The process of thermal conductivity in the volume of the blank, limited area Ω, with surface $\partial\Omega$, described by a scalar temperature field $T = T(P,t)$, vector heat flux field $\vec{q} = \vec{q}(P,t)P = \{x, y, z\} \in \Omega$ and a scalar field of specific thermal energy $e = e(T)$.

According to the research covered in [11], these fields are generated by sources W_s, depend on effluents W_g heat removal (due to hydrodynamic influence) from the surface $\partial\Omega$ according to Newton's law and heat transfer by gas flow with velocity $\vec{v}_f$ in the direction of the axis $0x$.

The law of conservation of thermal energy for any area $\omega \subset \Omega$ expresses the equality of energy released by heat sources W_s for a period of time $t_2 - t_1, t_2 > t_1 \geq 0$, the amount of energy consumed by the effluent W_g, spent on increasing internal energy e, energy transferred by heat streams $\vec{q}_T$ through the surface $\partial\omega$ for the same period of time and energy carried by the flow of gas and liquid at a rate $\vec{v}_f$.

$$\int_{t_1}^{t_2}\int_{\omega} W_s dvdt = \int_{t_1}^{t_2}\int_{\omega} W_g dvdt + \int_{\omega}\left[e(t_2) - e(t_1)\right]dv \times$$

$$\times \int_{t_1}^{t_2}\int_{\partial\omega}\left(\vec{q}_T + c_g + \rho_g T\vec{v}_f, \vec{n}\right)dsdt. \qquad (12)$$

Here dv and ds – volume and surface elements; $\vec{n}$ – ort external normal to $\partial\omega$; $(\vec{q}_T + c_g\rho_g T\vec{v}_f, \vec{n})$ – scalar product of vectors; $\vec{q}_T + c_g\rho_g T\vec{v}_f$ i $\vec{n}$; c_g i ρ_g – heat capacity and gas density.

Equation (12) can be recorded as:

$$\int_{t_1}^{t_2}\int_{\omega}\frac{\partial e}{\partial t}dvdt = \int_{t_1}^{t_2}\int_{\omega} g dvdt - \int_{t_1}^{t_2}\oint_{\partial\omega}\left(\vec{q}_T + c_g\rho_g T\vec{v}_f\right)dsdt.$$

Since integration occurs over an arbitrary period, we have:

$$\int_{w}\frac{\partial e}{\partial t}dv = \int_{\omega} g dv - \oint_{\partial\omega}\left(\vec{q}_T + c_g\rho_g T\vec{v}_f, \vec{n}\right)ds.$$

The last expression is the integral equation of thermal energy balance in a voluntary domain $\omega \subset \Omega$.

As an area $\omega \subset \Omega$ voluntary, then the last equation holds if the subintegral expression is zero

$$e_t + div\vec{q}_t + c_g\rho_g div(T\vec{v}f) = g, P \in w \subset \Omega, t > 0.$$

The last equation is the differential equation of thermal energy balance at a point $P \in \Omega$. This is a differential equation in partial derivatives. It contains an operator div over vector field $\vec{q}_T + c_g\rho_g T\vec{v}_f$ and the time derivative of the internal specific thermal energy e.

Equation of the balance of matter in a voluntary domain $\omega \subset \Omega$ using the Gauss-Ostrogradsky formula we can write

$$\int_{\omega}\left[mC_t + div\vec{q}_c + div\left(C\vec{v}_f\right)\right]dv = -\int_{\omega} f.$$

By virtue of the basic lemma of variational calculus for a voluntary domain $\omega \subset \Omega$ this equation is valid only if the subintegral expression is zero

$$mC_t + div\vec{q}_c + div(C\vec{v}_f) = -f, P \in \Omega, t > 0.$$

We have the Diffusion Equation at any point $P \in \Omega$ [11].

Temperature distribution on the surface under the action of a cylindrical concentrated energy source of radius r can be considered as the temperature field in the thickness plate h with dimensions significantly exceeding the thickness that stands still on the base. We will consider that heat extends to the moment when on a surface there will be a contact with the heat carrier which intensively dissipates heat - that is the area of heat removal is limited by radius R. Mathematical model, which allows to study the temperature distribution, leads to the solution of the next initial-boundary value problem for the equation of thermal conductivity

$$\Delta u - \frac{1}{a^2}u_t = 0, R_1 < r < R, 0 < \phi < 2\pi, t > 0, u(r,\phi,0) =$$

$$= u_0 R_1 < r < R, 0 < \phi < 2\pi,$$

$$\left.\frac{\partial u}{\partial r}\right|_{r=R} = F\left(\phi, t, u\right), \omega t < \phi < \omega t + 2\pi, t > 0,$$

$$u(r, \phi + 2\pi t) = u(r, \phi, t), R_1 < r < R, 0 < \phi < 2\pi, t > 0,$$

where $\Delta = \frac{1}{r}\frac{\partial}{\partial r}\left(r\frac{\partial}{\partial r}\right) + \frac{\partial^2}{\partial z^2} + \frac{1}{r^2}\frac{\partial^2}{\partial\phi^2}$ - differential operator in a cylindrical coordinate system (r, f, z); $a^2 = \frac{\lambda}{c\rho}; \lambda -$ heat conductivity coefficient; $c -$ heat capacity, $\rho -$ the density of the processed material. Then

$$F(\phi, t, u) = \begin{cases} q, \omega t < \phi < \phi_0 + \omega t \\ k\left(u_c^4 - u^4\right), \phi_0 + \omega t < \phi < \omega t + 2\pi \end{cases}$$

where $k = \frac{\varepsilon\sigma}{\lambda}$, ε – degree of blackness; σ – Stefan-Boltzmann constant; $u_c -$ ambient temperature; R, R_1 – radii of the outer and inner surfaces of the cylindrical zone of influence. As a result, we obtain a linear initial-boundary value problem for conjugation:

$$\frac{\partial^2\tilde{u}}{\partial\phi^2}-\frac{1}{\tilde{\tilde{a}}^2}\frac{\partial\tilde{u}}{\partial t}-b\tilde{u}=bu_c,\phi_0+\omega t<\phi<\omega t+2\pi,$$

$$\tilde{u}(\phi,0)=\begin{cases}d,0<\phi<\phi_0\\e,\phi_0<\phi<2\pi\end{cases},\tilde{u}(\phi+2\pi,t)=\tilde{u}(\phi,t),t>0,$$

$$\tilde{u}\big|_{\omega t+\phi_0-0}-g\frac{\partial\tilde{u}}{\partial\phi}\bigg|_{\omega t+\phi_0+0}=h\frac{\partial\tilde{u}}{\partial\phi}\bigg|_{\omega t+\phi_0+0}=g\frac{\partial\tilde{u}}{\partial\phi}\bigg|_{\omega t+\phi_0+0},t>0,$$

$$\tilde{a}=\frac{2(\ln R-\ln R_1)}{R^2-R_1^2}a^2,\omega=\frac{Rq}{\ln R-\ln R_1},$$

$$\bar{a}=2\frac{\ln R-\ln R_1+\mu_{11}(\gamma,R_1,R,k,u_c)}{R^2-R_1^2+2\upsilon_1(\gamma,R_1,R,k,u_c)},$$

$$b=\frac{4Rku_c^3}{\ln R-\ln R_1+\mu_1(\gamma,R_1,R,k,u_c)},$$

$$e=u_0+\frac{2q}{R+R_1\nu(\gamma,R_1,R)},$$

$$d=u_c+\frac{\left(R^2-R_1^2\right)(u_0-u_c)}{R^2-R_1^2+2\upsilon_1(\gamma,R_1,R,k,u_c)},$$

$$h=q\frac{(R-R_1)\mu(\gamma,R_1,R)}{\gamma(\ln R-\ln R_1)},\qquad(13)$$

$$\mu_1(\gamma,R_1,R,k,u_c)=4\frac{R-R_1}{\gamma}ku_c^3u(\gamma,R_1,R),$$

$$\upsilon_1(\gamma,R_1,R,k,u_c)=4\frac{R-R_1}{\gamma}ku_c^3\upsilon(\gamma,R_1,R).$$

Equipment,methods and sequence of research

To assess the effectiveness of the proposed hybrid processes used a universal laser-jet complex LSK-400-5, designed for controlled action on materials with high-intensity energy flows (including heat). The complex is described in detail in [12]. The general view of the complex is shown in Fig. 7, *a*, *b* and the main technical characteristics are given in table.3. Structurally LSK-400-5 consists of several subsystems interconnected and connected into a single unit by automation.

To create a stream of water ice cubes used the original device with flow control, the scheme of which is shown in Fig. 7, *c*. At the same time, the rational dimensions of the device elements and flow rate coefficients were determined by involving additive processes – 3-D printing means, which were used to make internal inserts of the device, nozzle attachments, etc., the mixing chamber by a flexible pipe with a flow regulator, which allowed to perform debugging with a sample of 1.20 g/s.

a *b*

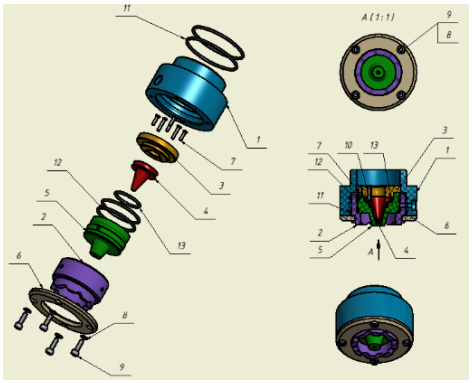

c

Fig. 7. Research complex LSK-400-5 (*a*, *b*) and the original device (*c*)

Table 3. Technical characteristics of the universal laser-jet complex LSK-400-5

№	Main data	Size	Parameter
1	Hydraulic drive power	kW	40
2	Maximum operating pressure	MPa	380
3	Pressure fluctuations at maximum power, not worse	%	9
4	Number of controlled coordinates		5
5	Number of simultaneously controlled coordinates		3
6	Desktop dimensions	mm	1500x2000
7	Laser type and beam wavelength	nm	Yag:Nd, 1062
8	Emitter power is average	W.	410
9	Pulse frequency	Hz	50–1000
10	Accuracy of working off of displacements	mm	±0,05
11	Fractionality of the abrasive	mm	0,05…0,22
12	Maximum fluid consumption	cm^3/min	45
13	Nozzle diameters d_c and a calibration tube D_k	mm	$d_c = 0,1...0,6$ $D_k = 0,8...1,3$
14	Total power	kW	45

Cryogenic liquid (liquid nitrogen) was fed to the mixing chamber by special pipelines, pre-cooled to a temperature of 250 K, the fluid flow was regulated using a slot-controlled throttle. Visual examination of the shape and size of ice particles to determine the fractionality was performed using an optical microscope LOMO BMI-1, equipped with CCD-type converter DEM-130, CMOSchip. Image multiplicity – up to x80.

Nozzles were made by prototyping on the designed 3-D models of photopolymer, bringing the roughness of the inner edge to R_a 6.3 μm. The transparency of the nozzle also allowed to observe both the quality of further refinement of the channel, and the resulting violations in the flow.

Since the narrowing of the cross-section and the transition from the cylindrical flow to the profile in length l = 22,0 mm caused the emergence of vortex zones, it was decided to install in the calibration part of the channel a special deturbulator - a flow rectifier, which is a package of cylindrical tubes of small diameter (d_t = 0,75 mm). This managed to solve two problems: 1) to ensure maximum "transparency" of the jet for laser radiation; 2) reduce the instrumental error of radiation intensity measurements. Establishment of temperatures as controlled values in the zone of formation of the water-ice jet was carried out with a pyrometer type ThermoSpot XP, with the limits of temperature determination – 80°C…+ 650 °C.

To establish the strength of the ice was based on the statement [10] that the latter is due to the degree of freezing T_z: $\sigma_l^{sg}(T_z) = (-0,7375 - 0,859T_z)10^6$, that is, determining the temperature at the point of contact with the surface (at a distance L_p from a cut of a nozzle), established not only the value σ_{kr}^*, but also the intensity of heat extraction from the jet stream. So proceeded from the condition of heat balance, i.e. the fact that the amount of heat Q coming to the ice from the environment is spent on heating the ice to the melting point and its transition from solid to liquid state is defined as $Q = Q_n + Q_a = cmT_z + L_p\rho h$, and from the Fourier provisions on heat equations, taking into account heat runoff $Q = Idxdydz\tau$, where I – the intensity of heat transfer from the environment to the ice; $dxdydz$ – elementary volume of the ice, in the first approximation (if $dxdydz = W_k$ and $\rho hs = m$) we have $T_z = \dfrac{lW_k\tau - L_p m}{cm}$ from where

$$I = \frac{T_z cm + L_p m}{W_k \tau} \qquad (14)$$

where c – specific heat of the ice; m – its average mass;

ρ – fluid density; L_p – specific heat of ice melting; h – crystallization layer over a period; s – ice surface area, τ – the time of movement of the ice by the slice is determined from the average speed of the water-ice flow.

Since during the theoretical research a hypothesis was formulated about the dependence of ice generation on the jet leakage conditions determined by the Reynolds number Re, the latter was established by the equation $\mathrm{Re} = \dfrac{\mu R}{\upsilon}\sqrt{2\dfrac{\Delta p}{\rho}}$ at the average velocity of the liquid in the nozzle space $\upsilon = \mu\sqrt{2\dfrac{\Delta p}{\rho}}$, known fluid viscosity, and the calculated nozzle flow rate as $\mu = \dfrac{Q_в}{\omega_t\sqrt{2\dfrac{p_b}{\rho}}}$.

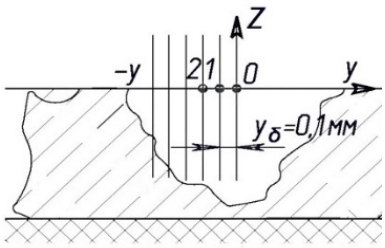

Fig. 8. Formation of the funnel of destruction of the composite layer

The distribution of velocities over the cross section of the jet was determined based on the measurement of the profile of the control volume of the material (Fig. 8) with perpendicular flow of the jet on the surface for a short period of time, using Finney's reasoning [13] relative to the volume removed from the surface due to deformation wear $\delta w_i = \dfrac{mv_i^2}{\psi\sigma_f}\left(\dfrac{\cos^2\alpha}{6}\right); \alpha \approx 0$, that is $h_i = Cmv_i^2;$, $\alpha = 0$ where m – mass consumption of particulars, C – the constant of the material, which determines its viscosity; σ_f – compressive strength of the material; v_i – the speed of the analyzed package of water-ice jet. Accepted $v_i \approx v_{ic}$.

The average value of the kinetic energy possessed by the jet was determined by the measured dimensions of the ice cubes, their number, taking into account the geometric parameters of the jet:

$$K = \frac{m\bar{v}^2}{2} = \frac{\bar{v}^2}{2}\frac{\pi\rho H}{3}\left(\frac{d_c^2}{4} + R^2 + R\frac{d_c}{2}\right) =$$

$$= \frac{\pi\rho H}{24}\left(\frac{d_c^2}{4} + R^2 + R\frac{d_c}{2}\right)v_c^2(1+k_p)^2,$$

where $k_p = \dfrac{d_c^2}{4\left[\dfrac{d_c}{2} + H\sin\left(\dfrac{\phi}{2}\right)\right]^2\cos^2\delta}$. A piece of ice was considered a round body that had a certain length l_a and diameter D_a, and calculated the volume of such a body by

the equation: $W_a = \frac{\pi D_a^2}{4} \cdot l_a$ The average mass of a particle is the density ρ was: $m_a = \rho \cdot W_a$. For average particle volume $W_a = 0,0020...0,0023$ mm^3 the mass of the particle was (at $\rho = 1,0$ g/cm^3) $m_a = 7...9$ mg.

The connection of the liquid jet with the laser beam was performed using a device with a coaxial nozzle, which allowed to form such an effect without the use of optically transparent elements of the mixing chamber.

To determine the distribution of radiation intensity and the formation of parameters on the irradiation surface $\delta^{pl}{}_{\iota}$, $\Delta^{ll}{}_{i}$, h_{σ}, l_j, designed and manufactured optical-jet stand, the schematic diagram of which is given in Fig. 9. The device allows: to determine the cost characteristics of the nozzles used to calculate the Reynolds number; use nozzles with different configurations of the channel profile and, accordingly, the coefficients of fluid flow μ; to form cross-sections of the jet with ring nozzles of a given cross-section, sufficient for observation without the use of a special optical system and magnifying equipment; change jet height - parameter l_s, and adjust the point of introduction of focused laser radiation by distance l_0; to carry out visual control and fixing of a configuration of a stream and its imprint, with use of the registering phototechnics. A flat surface was chosen as the main element E_1 that have dimensions 25.0x50.0 mm, thickness 10.0 mm; materials such as KIMF and UGKM carbon fiber.

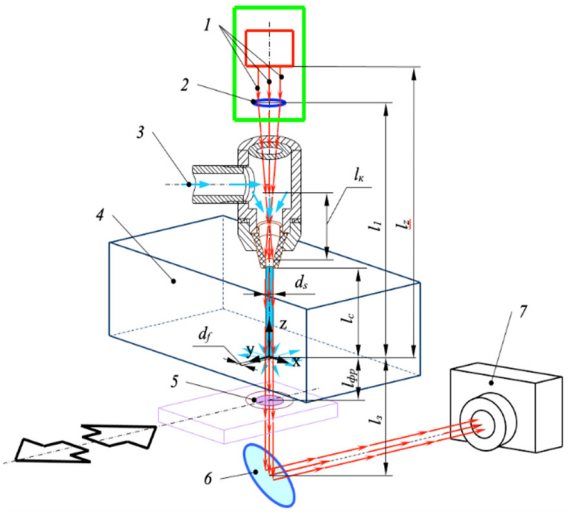

Fig. 9. Schematic diagram of a device for establishing the conditions of connection of a laser beam with a coaxially formed jet

Nozzle attachments were constructively designed so that the inlet area of the hole provides compensation for misalignment Δd_c laser beam and the formed jet of liquid and provided full reflection of a laser beam due to lack of its maximum reflection on borders of environments (liquid - air) at introduction into a nozzle space of the annular channel in diameter d_p. For convenience of visualization in installation the source of laser radiation of low power BGP-3010 – the solid-state laser with diode pumping (Diode Pumped Solid State Laser) was used. Diode radiation – 808 nm. The laser beam is focused and fed to Nd: YVO_4 – a crystal that converts from 808 nm to 1064 nm beam, followed by conversion of crystalline titanium phosphate, potassium, $KTiOPO_4$, double the frequency – 532 nm.

Using an experimental setup, the jet-laser effect on the non-conductive surface was simulated. Polymethyl methacrylate (plexiglass) was used as the latter. Considering its optical properties (transparency) during the experiment was recorded not only the magnitude of the luminous flux of the laser radiation source (using a photoresistor FSD-1 [14] Fig. 3.6 (Table 3.2)) depending on the height of the liquid column, but also the light configuration inkjet print (Canon Power Shot A110 digital camera has a 10MP matrix resolution). Also during the research, a transparent substrate was used, on the surface of which a grid with a step of 0.5 mm was applied, for the convenience of controlling the geometry of the same print.

The speed of fluid flow at the inlet of the nozzles is 14...50 m/s. Since the experiments showed a significant effect of pressure instability on the indicators of the recorded characteristics, the power supply system provided for the installation of an additional expander (accumulator), which partially smoothed the pressure ripples. Also, necessary when setting up research tools for the alignment of the jet of a low-power laser with a nozzle hole. AQUAPRESS AFC24SBA was installed in the liquid supply system to increase the accuracy of measurements. Given the possible differences in the measurement process, to record the measurement results, it was decided to use the m-DAQ ADC.

Since the intensity distribution and efficiency of laser-jet hybrid tool treatment depends on the flow conditions on Re, a method for determining Re when removing the characteristics of the jet flow formed by the profiled nozzle.

Thus, according to [15], the Reynolds number for the nozzle channel will be determined: $\mathrm{Re} = \frac{\upsilon R}{v}$ υ – the average speed of the fluid in the pipeline or in the channel; R – hydraulic radius; v – kinematic viscosity of the fluid.

In this case, for nozzles of complex cross-section, including ring, the critical value of Re will be up to 1000–1500. The distribution of velocities in the cross section of the channel is $u = \frac{1}{4} \cdot \frac{ig}{v}\left(r_0^2 - r^2\right)$ or after transformations, $u = \frac{gir_0^2}{4v}\left(1 - \frac{r^2}{r_0^2}\right)$ where g – Acceleration of gravity; i – piezometric slope; r_0 – radius of the pipeline.

Average velocity of the liquid in the nozzle space will be: $v = \mu\sqrt{2\frac{\Delta p}{\rho}}$, number $\mathrm{Re} = \frac{\mu R}{v}\sqrt{2\frac{\Delta p}{\rho}}$.

Focusing of the beam was performed according to the traditional method, checking the centering of the beam and the correct hit of all its modes on the focusing lenses of the tube. Blowing of the impact zone was performed with ordinary compressed air, which entered the nozzle with a diameter of 2.8 mm at an excess pressure of 0.05 MPa; the air was filtered and came from the receiver. The liquid was supplied from a nozzle with a diameter of 1.5 mm directly to the center of focus of the laser. The working feed to obtain a groove of 2.0 mm was set at 300 mm/min., The laser head was given a rectilinear motion, and the distance between the nozzle cut and the cut surface was set provided the location of the focal plane on the plate surface, ie at a distance of 7.2 mm.

Research results and their discussion

Hybridization of the tool, based on the interaction of different mechanisms and essence of the processes, is performed based on the results of modeling of different influences (1–6), the basic laws of which are given above. Usually, hybridization of the effect is possible listed in table 1: M_r, M_d, L, WJ, Ab, Cr. Since $N = 6$, variants of combinations $N! = 720$. Strictly speaking, this is the maximum number of options for influence, which involves a certain sequence of factors. However, hybridization reduces this amount because: in the general case, the sequence of sampling of the combination is not important; there are options for combining influences with 2–3 or more actions. Then, for $N = 6$ and combinations of $m = 2$ action, the number of combinations is: $C_n^m = \frac{n!}{(n-m)!m!}$, that is $C_6^2 = 15$. This is a much smaller number, and for three options $C_6^3 = 20$.

Thus, such a limited number of effects allows you to create a table comparing treatment options, which is based on the search for options table. 1 from the condition of ensuring the cost of treatment, table 2.

Here are some simulation results for solving problems of practical importance.

Conclusions

The methodology and bases of creation of hybrid highly effective tools for processing of composite materials are developed. It is shown that the application of principles and approaches to identify rational methods of action on the processed material can significantly change the depth of penetration of technological action from the macro level to the microlevels, and in some circumstances – to the nanozones of influence.

The practical application of the proposed approach to the creation of surface treatment tools (in particular, for cleaning surfaces and removing the surface layer) and for cutting operations of composite materials is considered. Variants of realization of influences are resulted and their comparison is performed.

It is shown that cleaning with a hybrid tool that combines water-ice impact with mechanical initiation of initial defects of non-rigid hollow base surfaces is 25–40% higher compared to typical technical solutions. Cutting composite materials by laser-jet method is expedient in the treatment of high-strength compounds. The greatest expediency is seen in the treatment of multilayer compositions, for which it is possible to perform curved cuts with a roughness level of R_a 6.3 μm to a depth of 10 mm.

References

[1] Ye.I. Golibardov, A.V.Kudryavtsev and M.I. Sinenko, *Tekhnika FSA*, Kyiv: Tekhnika, 1989.

[2] B.M. Bazrov, “Sovershenstvovaniye proizvodstva detaley na osnove modul'noy tekhnologii”, *Tekhnologiya priborostroyeniya* Vol. 4. TS-9, p. 52, 1989.

[3] V.S. Ivanova *et al*., *Synergetics and fractals in materials science*, Moscow: Science, 1994.

[4] O.F. Salenko, I.V. Petko and O.V. Tret′yakov, *Hidro-ta hidroabrazyvna obrobka: teoriya, tekhnolohiya ta obladnannya*, Kyiv: IZMN, 1999.

[5] M. Hashish, “Steel Cutting with Abrasive Waterjets,” *Proceedings of the 6th International Symposium on Jet Cutting Technology,* BHRA, Surrey, England, pp. 465–487, Apr. 1982.

[6] S.A. Klimenko, Yu.A. Mel’niichuk and G.V. Vstovskii, “Interreation between the Structure Parameters, Mechanical Properties of Sprayed Materials, and the Tool Life in Cutting Them”, *J. of Superhard Mat*, Vol. 30, No. 2, pp. 115–121, 2008.

[7] P.D. Gindin, “Mathematical model of thermal decomposition of brittle anisotropic materials”, *Surface*. No. 1, pp. 14–18, 2010.

[8] O. Salenko *et al*., “About some results of treatment SiC-microarrays by Hydroabrasive Precision Jet”, *Journal of Mechanical Engineering NTUU* “*Kyiv Polytechnic Institute*”, pp.178–184, 2013.

[9] I.O. Povkh, *Tekhnicheskaya gidromekhanika*, Moscow: Mashinostroyeniye, 1976.

[10] M.A. Burnashov, A.N. Prezhbilov and YU.V. Vasilenko, “Modelirovaniye protsessa razrusheniya pokrytiya vodoledyanoy struyey pri ochistke detaley mashin”, *Vestnik YUUrGU. Seriya* “*Mashinostroyeniye*”, Vol. 17, No 2, pp. 67–73, 2017. DOI: 10.14529/engin170208.

[11] W. Schulz *et al*., “Simulation of Laser Cutting”, *The Theory of Laser: Mat. Proces*, JohnDowden. Springerpb., No. 119, pp. 21–69, 2009.

[12] A.F. Salenko, V.T. Shchetinin and A.N. Fedotyev, “Improving accuracy of profile hydro-abrasive cutting of plates of hardmetals and superhard materials”, *J. ofSuperhardMat*., Vol. 36, No. 3, pp. 199–207, 2014.

[13] M. Hashish, “Three-dimensional machining with abrasive-Waterjets”, in *Jet Cutting Technology. Fluid Mechanics and its Applications*. A. Lichtarowicz Ed., Dordrecht: Springer, pp. 605-620, 1992. DOI: 10.1007/978-94-011-2678-6_40

[14] V.Yu. Kholodnyy and A.F. Salenko, “Primeneniye struyno-lazernogo metoda obrabotki dlya perforirovaniya sotovogo zapolnitelya aviatsionnykh sendvich-paneley”, *Eastern-European Journal of Enterprise Technologies*, Vol. 1/5 (79), pp. 19–30, 2016. DOI: 10.15587/1729-4061.2016.59870

[15] O. Salenko *et al*., *Jets methods of cutting carbide and super hard materials*, LAP LAMBERT Academic Publishing (2014-11-13).

[16] V. Tkachuk *et al*., “The hybrid action tool for operations of cleaning of turbine units cavities”, *Mech. Adv. Technol*., no. 2(89), pp. 79–90, Sep. 2020. DOI: https://doi.org/10.20535/2521-1943.2020.89.205168

[17] A.F. Salenko *et al*., “Methods of cutting for workpieces of hardmetal and cBN-based polycrystalline superhard material”, *J. of Superhard Mat*, Vol. 54, No. 6, pp. 78–96, 2015.

Використання функціонального підходу при розробці гібридних процесів у машинобудуванні: теоретичні основи

О.Ф. Саленко, С.А. Клименко, В.М. Орел, В.Ю. Холодний, Н.В. Гаврушкевич

Анотація. *Наведено принципи створення гібридних обробних процесів на основі функціонального підходу. Запропоновано розглядати формування окремих елементів виробу (площин, отворів, заокруглень, уступів) через функції, що забезпечуються сукупністю таких елементів. При цьому аналізується потрібна глибина технологічних впливів, на основі чого підбирається сукупність різних за природою, однак сумісних впливів, що базуються на певному носії. Таким носієм запропоновано використовувати високошвидкісний потік рідини. Гібридизація інструменту на основі водяного струменя малого діаметра може бути досягнута суміщенням з лазерним нагріванням, кріогенним охолодженням та формуванням потоку крижаних частинок, механічним ініціюванням поверхневих пошкоджень з подальшим розвитком поверхневих дефектів. Показано високу ефективність гібридних процесів для обробки композиційних матеріалів.*

Ключові слова: *гібридний інструмент, функціональний підхід, обробка композитів, лазерна обробка, струменево-лазерне різання, кріогенна кригогенерація.*